Lux junior 2024

17. Internationales Forum für den lichttechnischen Nachwuchs
Ilmenau, 6. – 8. September 2024
DOI (proceedings): 10.22032/dbt.61636

DOI: 10.22032/dbt.xxxxx

Identification, Localization and Classification of the Color VEP for Application in Color Science

Brandon Fobugwe, B.Sc., Julian Klabes, M.Sc., Dr.-Ing. Alexander Herzog, Prof. Tran Quoc Khanh

Technical University of Darmstadt, Laboratory of Adaptive Lighting Systems and Visual Processing

1 Abstract

Experimental research on the preference of a light stimulus still mostly relies on subjective feedback of participants which is why Electroencephalogram (EEG) recordings could meaningfully enrich those experiments by providing low-level psychological response data. There is little research on the influence of color on Visually Evoked Potentials (VEP) or the visual pathway regarding color perception and even less is known about visual processing with regards to color preference. This work shows that it is possible to both linearly separate EEG for differently colored stimuli as well as to spatially separate the VEPs with regards to different visual areas in the visual cortex all by employing a consumer-grade EEG device. High-luminance stimuli as well as the presented red stimuli produce higher peak VEPs than the produced low-luminance and green stimuli. Furthermore, the Color VEP seems to propagate from the primary visual cortex V1 towards the secondary visual cortex V2 which corroborates the assumptions of a hierarchical visual processing of color. This work was done in anticipation of further research which is meant to eventually find a link between color metrics, color preference and EEG features.

Index Terms: EEG, VEP, Visual processing, Color Preference

2 Introduction

Research in lighting technology and especially in color science is usually based on psychophysiological experiments whose results are described by subjective evaluations of the test subjects **[1] [2] [3]**. A person perceives a stimulus visually and assesses it regarding a specific visual task.

The underlying visual processing of the stimulus takes place at different locations in the human visual system. On the input side there is the retina, in which certain photons excite different types of cones, which then generate action potentials. The information is then encoded into red-green, blue-yellow and light-dark opponent channels [4]. At the other end of the processing chain stands the brain, which creates a certain color impression that can be represented in a color space (Figure 1) [5].

The transition from opponent-channel-dominated action potentials to color appearance has not been sufficiently researched. However, this transition must arguably be reflected in the neuronal activity of the brain.

Thus, in order to quantify a low-level neuronal response to a visual stimulus, it seems logical to analyze brain activity during an experiment. In this way, the knowledge gap regarding visual processing could be closed. An Electroencephalogram (EEG) constitutes a non-invasive option to record such neuronal activity which could prove to be a valuable addition to future experiments in lighting technology.

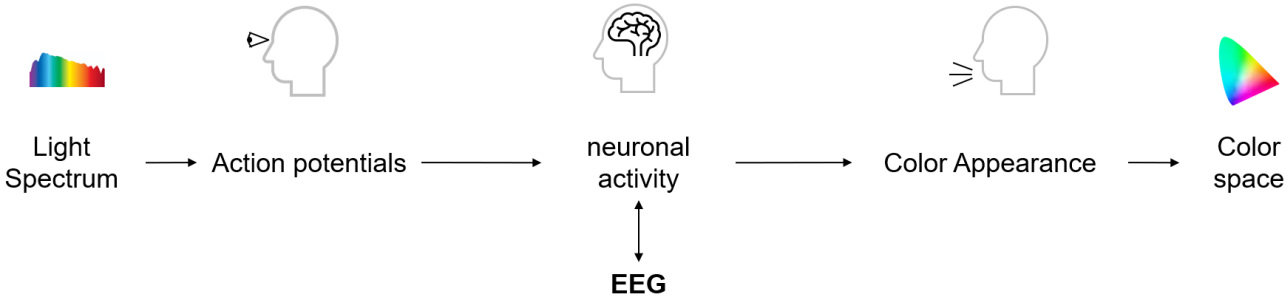

Figure 1: EEG might give insights in the processing of color information between color opponent encoding and color space.

2.1 Visual Processing

The entire visual cortex extends over large parts of the occipital lobe into the parietal lobe [4] (Figure 2). The visual signals first reach the primary visual cortex V1. at this point, according to the current state of research, the opponent channel representation still dominates [6]. In what way color is encoded in the neuronal

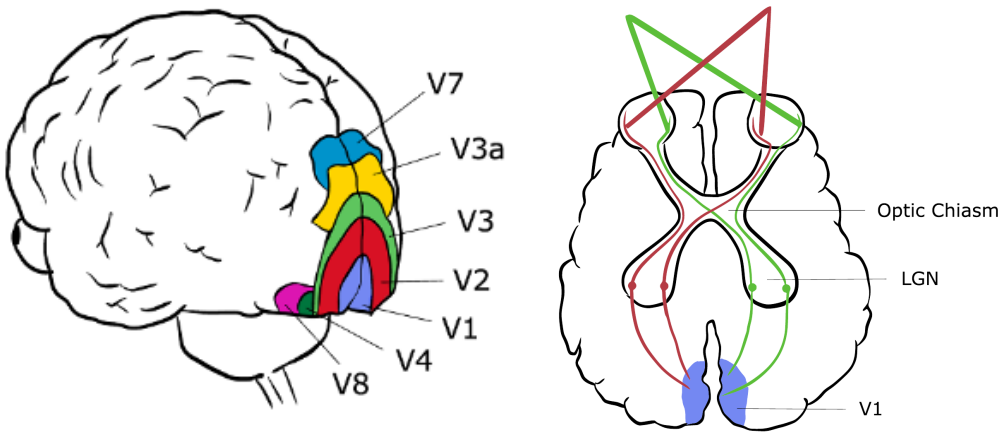

Figure 2: Action potentials from the two retina hemifields are combined in the optic chiasm (a). They pass the LGN in the thalamus and reach the primary visual cortex V1. Graphic adapted from [20] and modified. The human visual cortex lies in the occipital lobe at the back of the head (b). The primary visual cortex V1 is believed to receive information first. In the hierarchical color processing model, the information is passed through V2 towards the higher visual areas. Graphic adapted from [21] and modified.

signals from this point onwards is much discussed in the literature. There are various models of information processing within the visual cortex. The hierarchical model, for

example, describes sequential processing through V1 via V2, V3 and so on, whereby the complexity of the processed information of the visual stimulus increases steadily [6].

2.2 Visually Evoked Potentials

Visually Evoked Potentials (VEP) describe EEG potential changes which occur in response to a visual stimulus [7]. They are clinically defined and consist of different peaks in the time signal (Figure 3). The shape depends on the type of visual stimulus. Peaks are partly denoted using their orientation combined with the point in time at which they occur. P100 denotes a positive peak 100ms after stimulus onset, for example.

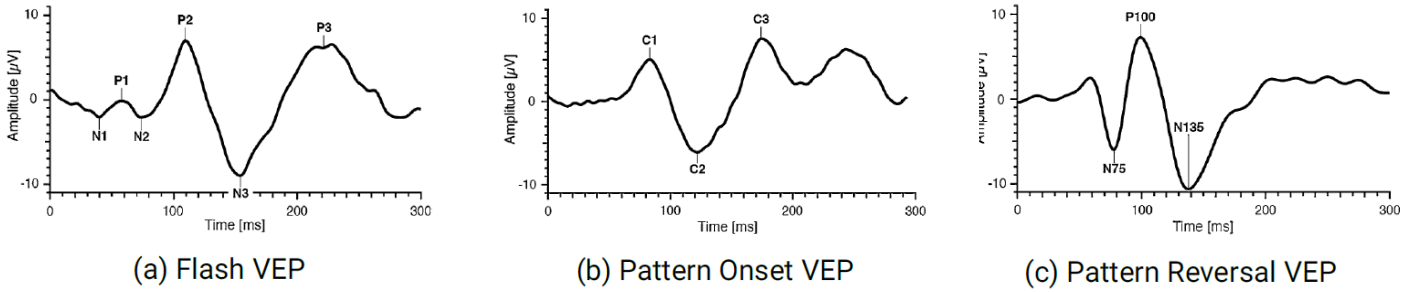

(a) Flash VEP (b) Pattern Onset VEP (c) Pattern Reversal VEP

Figure 3: VEPs as defined by the ISCEV 2016 standard. Graphic taken from [7].

3 Methods

This work used an EEG measurement system based on the OpenBCI platform. OpenBCI provides hardware and software that can be used to build relatively flexible and high-quality EEG systems [8].

This work's setup employs a 3D printed headset with active, dry electrodes screwed into it. The headset can be quickly installed without the need for time-consuming positioning of each electrode. A so-called Cyton data processing board from OpenBCI is mounted on top of the headset. It samples the EEG signals at 1000 Hz and sends them to a laptop via WiFi (Figure 4).

Another crucial part of this system is a photodiode which is attached to the monitor and electronically connected to the Cyton. It allows the recorded EEG signal to be precisely synchronized with the onset of a stimulus.

The setup uses dry electrodes. Unlike conventional EEG electrodes, no gel needs to be applied to the scalp. They are also active, meaning that the measured signal is amplified in the electrode head [9].

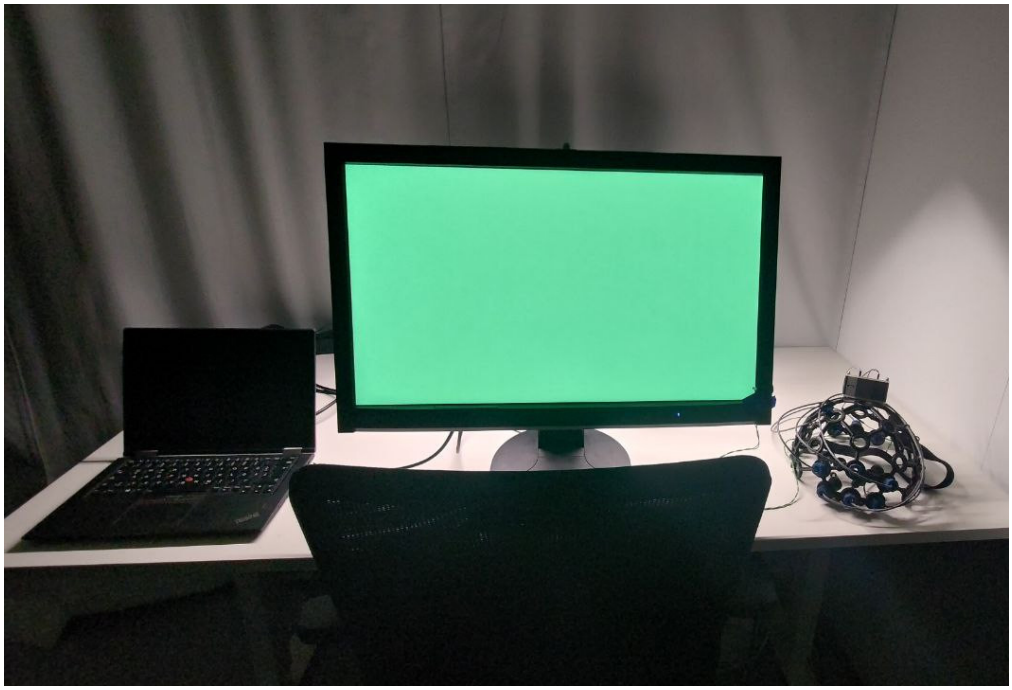

Figure 4: The experiment setup which is used in this work. The participant was seated and equipped with the headset which sent real time EEG data to the laptop.

The positions of the electrodes were chosen so that they cover the visual cortex. Three positions are assigned to the occipital lobe (O1, O2, Oz) and three others also cover parts of the parietal lobe (Po3, Poz, Po4). Roughly speaking, Oz corresponds to V1 and Poz to V2 [10]. This spatial distribution of the six electrodes is meant to enable tracking the VEP more precisely than with just one electrode. The main experiment of the work consists of changing the color stimulus on the screen with regards to a simple color metric and measuring the response of the visual cortex to this change. This is done for a change in luminance and a change in saturation respectively.

For the luminance experiment, the screen is changed from black to white at two different luminances. The white stimulus is held for one second before black is shown again. This is repeated 50 times, resulting in 100 trials for one experiment. The complete experiment is then carried out 7 separate times resulting in 700 trials. The saturation experiment is completed in the same way, except that a transition from gray to red or green is produced at a constant luminance. This results in a total of 350 time-synchronized EEG signals per experiment and per stimulus, which are referred to as trials in this paper.

4 Results

A single trial is shown as an example at the top of Figure 5. The gray shaded time spans mark the points in time before and after the stimulus was presented. Such single trials are very noisy and a VEP cannot be visually identified in the time signal. A robust method to remove noise from a group of time-synchronized signals is

across-trial averaging [11]. This involves averaging the signals across several time locked trials.

At an averaging batch size of 10 the VEP visually manifests and then reveals itself more clearly at higher averaging batch sizes (Figure 5). One can clearly visually identify an evoked potential at about 100ms after the onset of the stimulus. Similar to the onset, after offset of the stimulus, a small VEP can be identified as well. No activity is recognizable in the static phase between onset VEP and offset VEP after averaging.

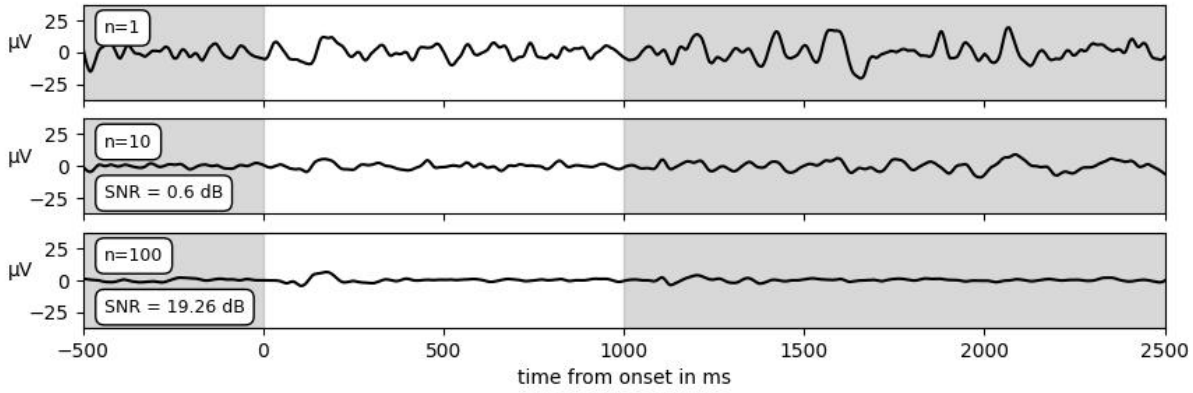

Figure 5: Across trial averaging facilitates visual inspection of the VEP. While the VEP cannot be visually identified in a single trial (row 1) the across trial averaging brings out the VEP shape. The example here was created using a gray-red transition. SNR was determined using the plus-minus-averaging technique [12].

4.1 Identification

For the luminance experiment, a clear VEP can be seen in all six measured positions (Figure 6). It manifests in two positive peaks and one negative peak. Interestingly, the SNR in the occipital channels is higher than in the parieto-occipital channels, which could indicate a higher information content in V1. The VEP of the high luminance can be characterized by a negative peak at 80ms and the lower luminance exhibits a negative peak at 120ms. A brighter luminance also seems to lead to a lower latency when considering the minimum of the VEP. P185 is significantly higher for the bright stimulus. The three peaks were defined to describe differences between the two VEPs, which is why, for example, this peak at 50 ms was omitted because it

does not differ greatly.

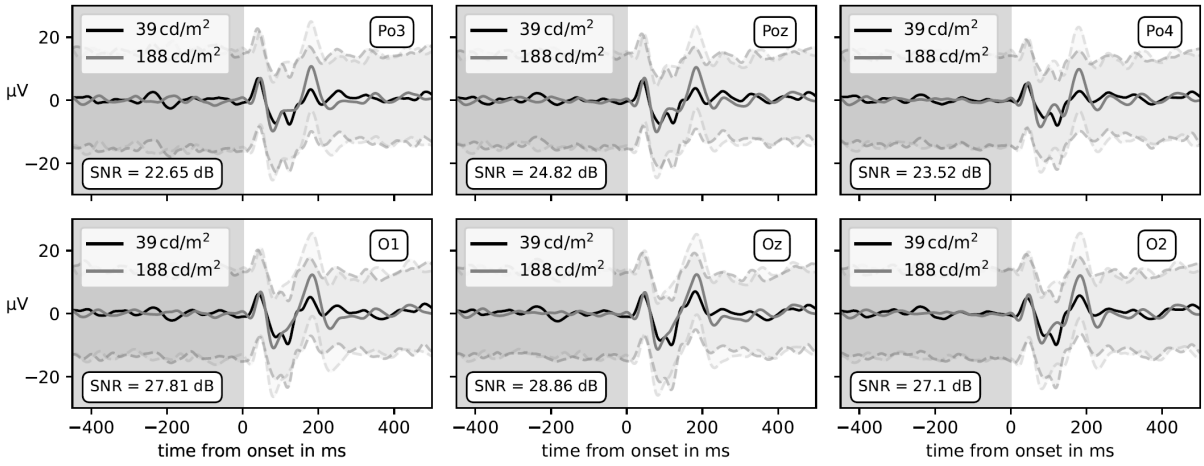

Figure 6: The VEP for an increase in luminance is clearly distinguishable in all six channels.

The increase in saturation also generates a VEP which is detectable in all channels (Figure 7). Merely Po4 does not exhibit a recognizable VEP, probably due to incorrect placement of the electrode in several experiments.

Interestingly, there is a double negative peak for this VEP. These two peaks could possibly be mixed from spatially distinct sources which will be investigated later in the localization section.

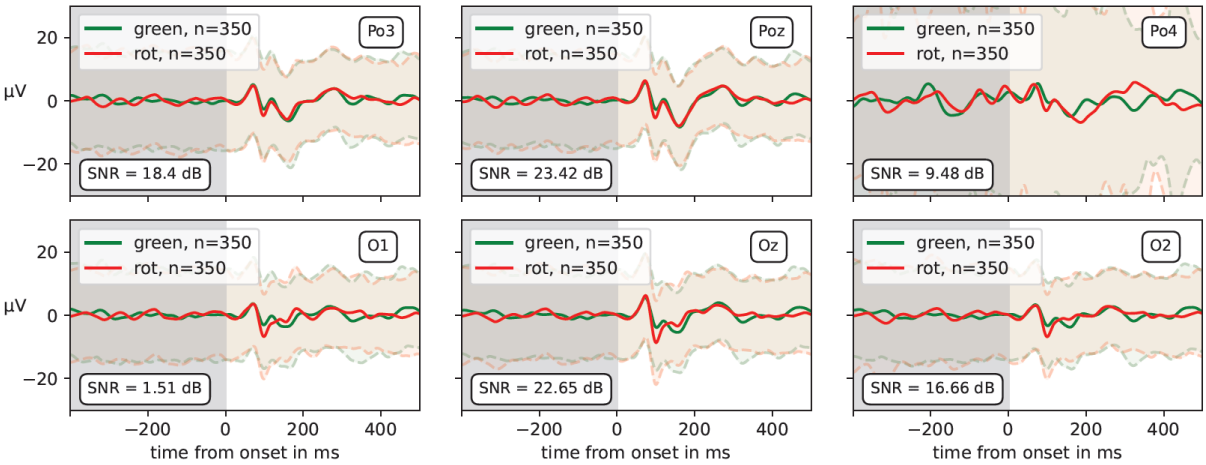

Figure 7: The VEP for an increase in saturation is also clearly visible. It is seemingly different for the two examined chromaticities.

Statistical comparison tests were conducted. There exist multiple features of the EEG signals which exhibit significant differences regarding different luminances and chromaticities. The exact results shall not be further discussed in this paper.

4.2 Localization

The measured potentials are spatially blurred because the EEG signals are measured through the skull. They are locally poorly resolved and always represent a mixture of different sources [11].

As already mentioned, the shapes of the VEPs suggest spatially distinct components of the VEP regarding the saturation experiment. Using independent component analysis (ICA), individual components can be determined from a set of mixed signals [13].

The VEP is assumed to consist of three components, namely two locally different components and a noise component. All 700 trials of the saturation experiment are averaged and then put into the FastICA Algorithm from scikit-learn [14] to determine three components. An earlier component seems to have its origin in V1 and a later one is mainly found in V2 (Figure 8). The scalp maps at the bottom of Figure 8, visualize the location of a component. The third component consists of artifacts that are likely related to channel Po4.

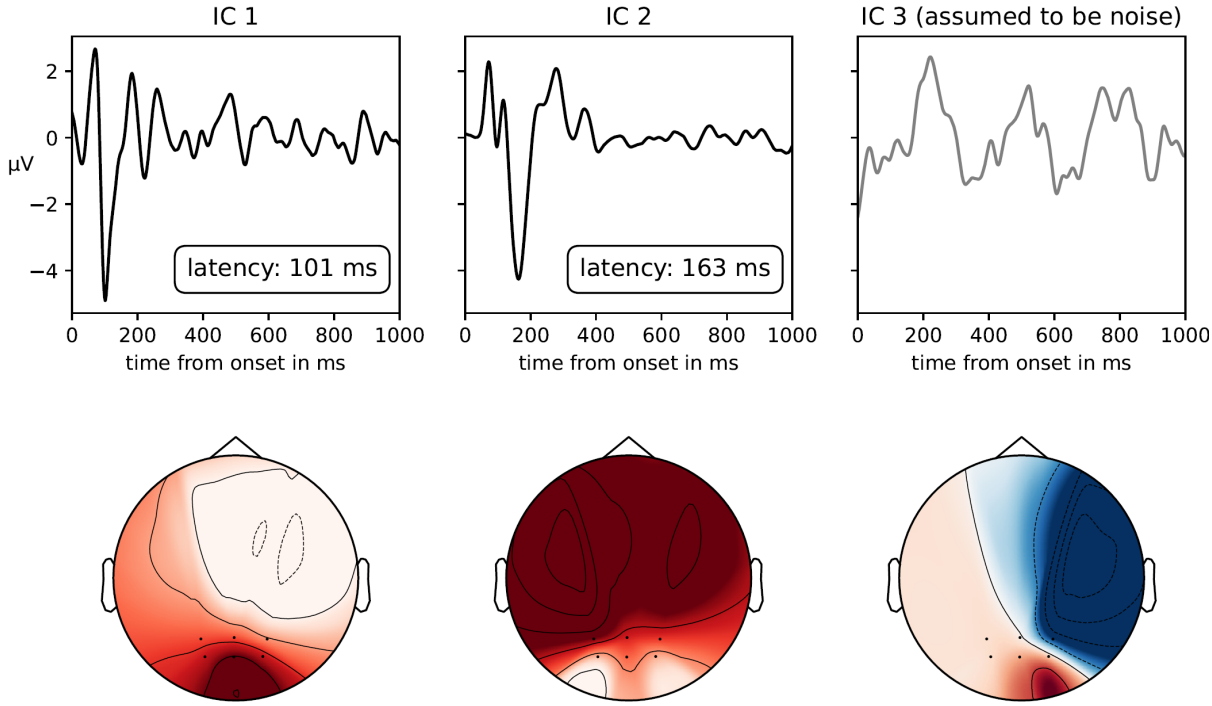

Figure 8: The Color VEP can be separated regarding individual independent components. There are two components corresponding to the occipital and parieto-occipital channels respectively.

4.3 Classification

By employing machine learning classification algorithms, it is now inspected whether the signals can be separated based on various features relating to the luminance or chromaticity of the stimulus. A simple classifier, namely a support vector machine (SVM) was chosen. This classifier considers the individual EEG signal features in a high-dimensional space of the various features and tries to find a hyperplane that separates the data points as well as possible [15].

First, it is of interest to find those features with which the classifier can most consistently be successfully trained. A feature selection algorithm, namely Recursive Feature Elimination (RFE) is used. This describes a feature selection technique that

successively eliminates features from training rounds until the trained model exhibits optimal accuracy [14]. In this work a cross validation based RFE from scikit learn is employed. The RFE algorithm uses an SVM without a kernel, i.e. a linear hyperplane. The features are calculated based on ten-fold averaged signals. This gives a list of optimal features. The algorithm is then repeated 50 times, and the selection frequency of the features is added up. This results in a selection frequency for all features. In total, the process was repeated 5 times to ensure that the results do not vary greatly.

Figure 9 shows the resulting feature selection frequency for the luminance experiment. The two peak features clearly seem to have the highest importance. Only the standard deviation shows a slightly increased importance as well.

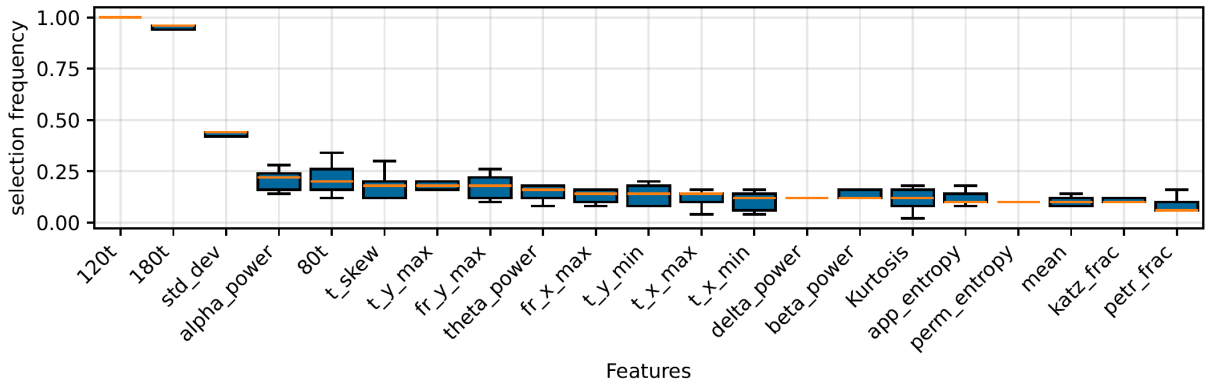

Figure 9: For classifying the luminance VEP both the amplitudes at 120 and 180 ms are most important.

For the saturation experiment, it can also be determined that the two defined features are best suited to separate the data linearly (Figure 10). However, it is noteworthy that some other features also achieve approx. 40% importance.

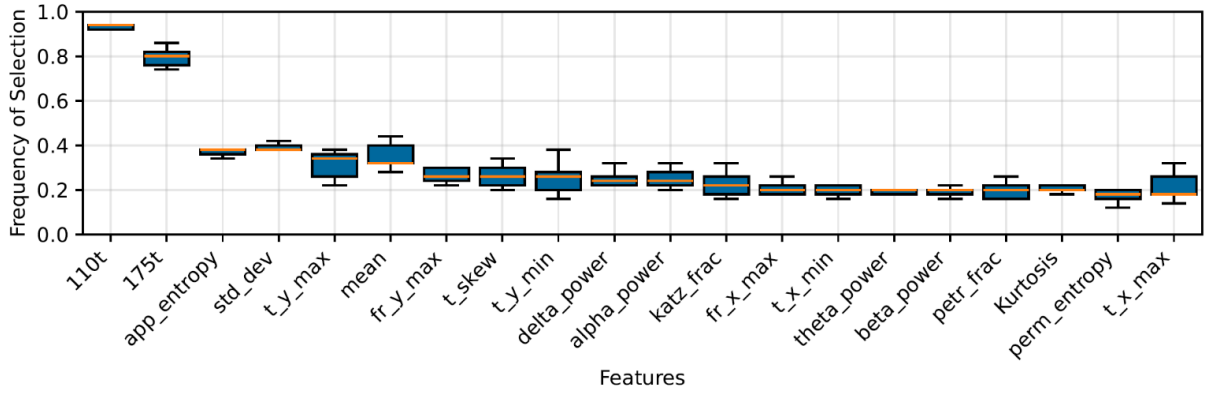

Figure 10: Amplitudes at 110 and 175 ms are both most important to classify the chromaticity regarding a change in saturation.

Since such a separation is possible with just two features and since the SVM uses a linear hyperplane, these decision boundaries can be visualized easily. For the illuminance experiment, a hyperplane that separates the training data by 90% is shown in Figure 11 on the left. The trials were averaged 10-fold. Based on the orientation of the hyperplane, it can be concluded that a high luminance means a more positive potential for P180 but also for N120. The skewness is therefore more positive for higher luminance, which also confirms the results of the statistical analysis.

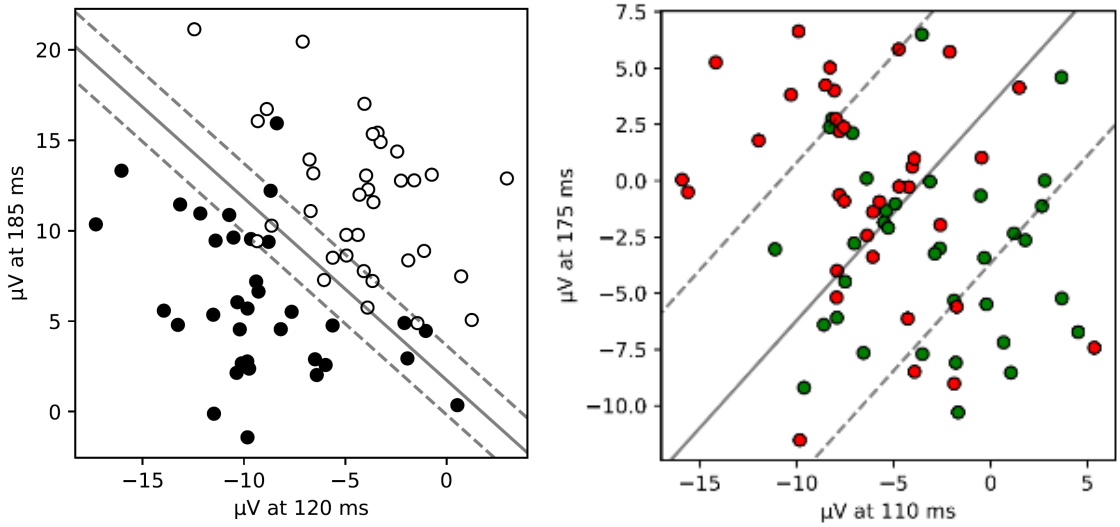

Figure 11: Exemplary Hyperplanes for classification of ten times averaged trials. The hyperplanes differ in orientation leading to different conclusions of the impact of different color metrics on the VEP.

Modelling the saturation experiment results in a different orientation of the hyperplane (Figure 11 on the right). The example separates the training data by 80%. However, the relevant difference seems to relate to the difference between the positive and negative peaks. Followingly, red stimuli seem to cause a more prominent VEP than the green stimuli.

The median performance of the linear SVM for the chromaticity experiment increases with the averaging batch size (Figure 12). Here, the cross-validated accuracy is shown in relation to the averaging batch size.

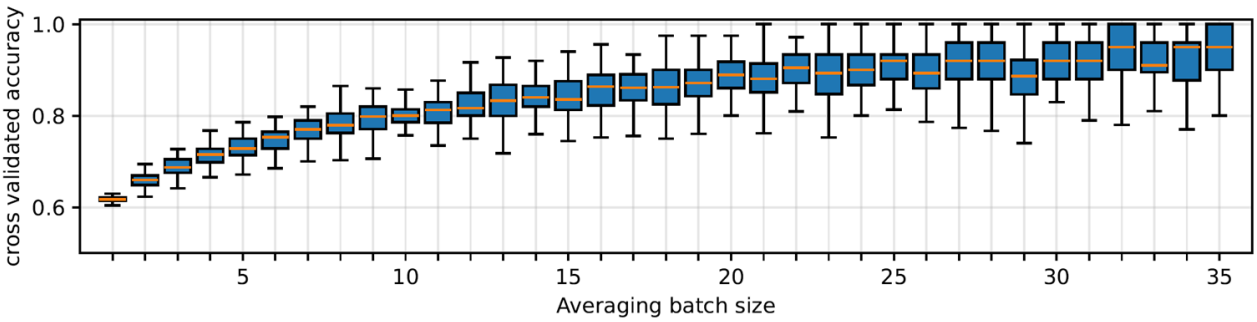

Figure 12: Accuracy over averaging batch size increases mostly monotonously.

The median accuracy increases steadily and reaches 73% for an average of 5 and 80% for an average of 10. This is roughly in line with results from Böck et al. who reached 83% accuracy with 10-fold averaging [16].

4.4 Exploratory Analysis: CNN for Color VEP classification

To improve the classification accuracy, a Convolutional Neural Network (CNN) is trained on a set of wavelet scalograms of the signals. These scalograms are the result of a continuous wavelet transform of 5-fold averaged trials and visualize the signal in the time and frequency domain [17]. The average scalograms for red and green VEPs are shown Figure 13. They visualize the average activity of the signals for a time range of 0 to 1s after stimulus onset. Red VEPs seem to cause a higher activity approx. 180ms after the stimulus is applied.

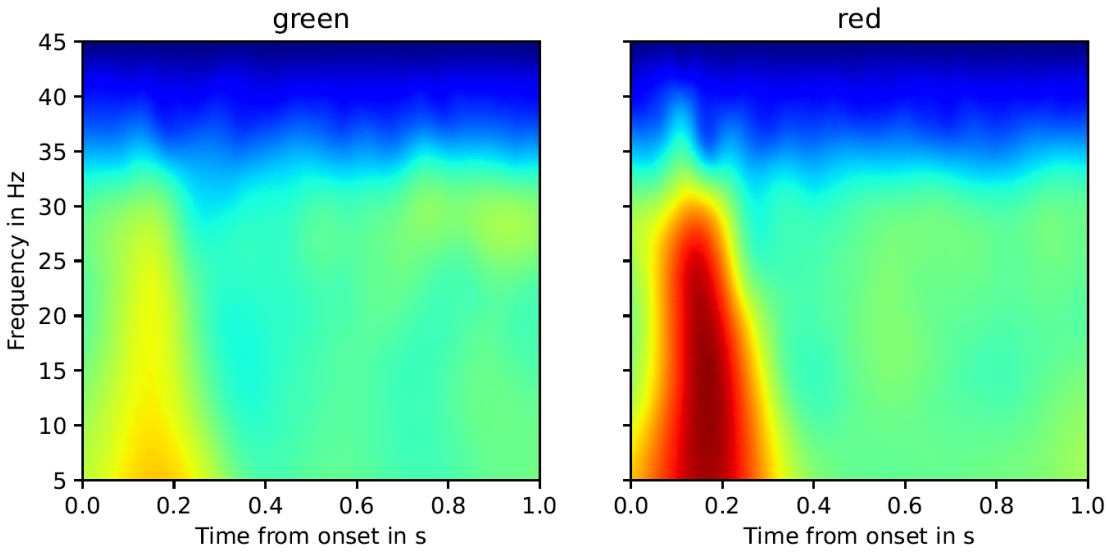

Figure 13: Average Scalogram of the green and red VEPs respectively. Red VEPs seem to exhibit a stronger activity after around 180ms.

A shallow CNN is trained on the dataset. It achieves a cross-validated accuracy of 83%. This is already notably higher than the 73% reached by the SVM. However, in contrast to an SVM, the interpretation of the model is somewhat more difficult here.

So-called saliency maps describe what part of an input image the CNN is looking at, in order to classify a specific image. In order to interpret the results, this work opted for a grad-CAM which describes the derivation of the model with regards to a certain input for a certain output class [18]. Figure 14 shows the average grad-CAMs of all scalograms. Notably, the maximum lies at approximately 180ms for both VEPs. The maximum for red VEPs is slightly shifted upwards. One could conclude that red VEPs are more strongly characterized by activity in higher frequency bands, i.e. higher than 15 Hz.

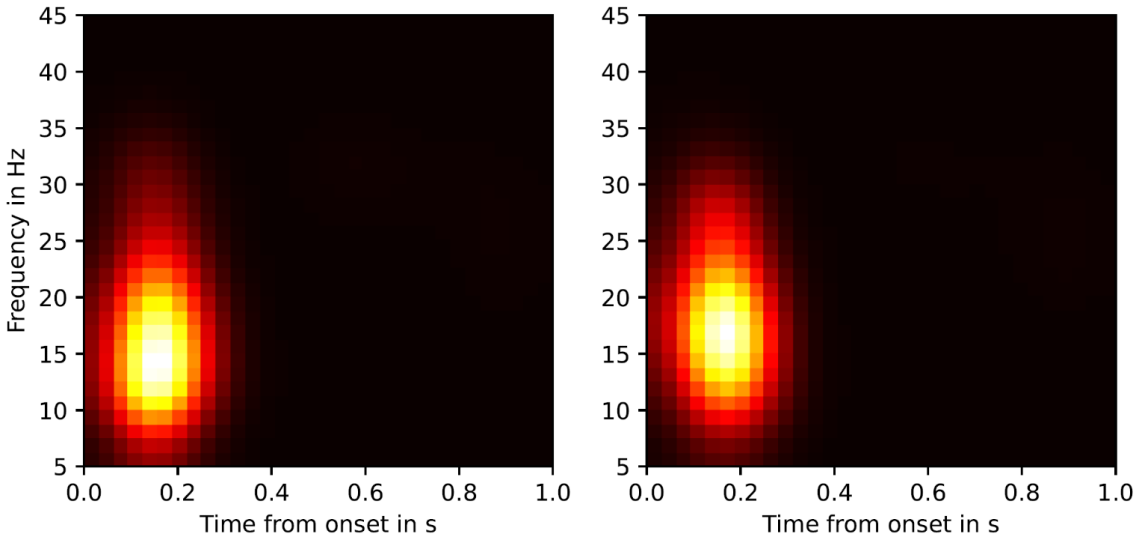

Figure 14: Grad-CAMs for green (left) and red (right) VEPs. The trained CNN seems to focus more on higher frequencies when classifying VEPs as red.

5 Conclusion

The color VEP can be detected with the described system setup, however, the noise must be strongly reduced, which is well achieved by across trial averaging, i.e. the averaging of time-synchronous signals. These VEPs can also be examined in detail with regards to the origin of individual components in the cerebral cortex. It is therefore possible to conduct research into visual processing in time and space. In addition, the signals can be separated linearly according to the stimuli they are produced by. This means that different colors cause different VEPs which then can be classified. Followingly, certain signal features can be linked to certain color metrics. However, static stimuli cannot be classified with this system. For this, other brain lobes or simply a higher number of channels would have to be measured. For instance, a pattern analysis based on a large-scale EEG measurement of the entire cerebral cortex is conceivable [19].

6 Future Work

Future work could investigate additional color metrics such as those based on the TM-30. It also seems logical to extend the EEG measurements to the entire cortex. While the VEP itself could be found in various test subjects, most of the statistical analysis relates to data of a single subject. Consequently, large parts of the work still need to be validated in other subjects.

Due to the possibility of investigating visual processing in both a spatial and temporal matter, future work could focus on the visual processing of color stimuli in the visual cortex.

Color distance experiments seem plausible as well. They could be used to create a color space that is uniform in terms of neuronal activity. Using EEG, these experiments could be conducted faster than in the traditional way.

7 Figures

8 References

[1] Z. Huang, Q. Liu, M. R. Luo, M. R. Pointer, Y. Liu, Y. Wang and X. Wu, "Whiteness and preference perception of white light sources: A case study at 5500 K with positive and negative Duv values," *Optik,* vol. 240, 2021.

[2] T. Khanh, P. Bodrogi, Q. Vinh and D. Stojanovic, "Colour preference, naturalness, vividness and colour quality metrics, Part 1: Experiments in a room," *Lighting Research & Technology,* vol. 49, no. 6, pp. 697-713, 2016.

[3] F. Zhang, H. Xu and H. Feng, "Toward a unified model for predicting color quality of light sources," *Applied Optics,* vol. 56, no. 29, pp. 8186-8195, 2017.

[4] M. F. Bear, Neurowissenschaften: Ein grundlegendes Lehrbuch für Biologie, Medizin und Psychologie, Springer, 2018.

[5] W. D. Wright, "A re-determination of the trichromatic coefficients of the spectral colours," *Transactions of the Optical Society,* vol. 30, no. 141, 1929.

[6] Z. Li, "A very brief introduction of what is known about vision experimentally," in *Understanding Vision: Theory, Models, and Data* , 2014, pp. 16-66.

[7] J. V. Odom, M. Bach, M. Brigell, G. E. Holder, D. L. McCulloch, A. Mizota and A. P. Tormene, "ISCEV standard for clinical visual evoked potentials: (2016 update)," *Documenta Ophthalmologica,* vol. 133, pp. 1-9, 2016.

[8] C. Weirich, Y. Lin and T. Q. Khanh, "Evidence for human-centric in-vehicle lighting: part 3—Illumination preferences based on subjective ratings, eye-tracking behavior, and EEG features," *Human Neuroscience,* vol. 17, 2023.

[9] C. Labs, "Dry and Flexible Active Electrode for EEG Measurement - Sensor Data Sheet.," 2020. [Online]. Available: https://drive.google.com/file/d/1Ri2UPmPH2SrTjYQ8Mj046ciWLGzRxCSl/view.

[10] A. Gialopsou, C. Abel, T. M. James, T. Coussens, M. G. Bason, R. Puddy, F. Di Lorenzo, K. Rolfs, J. Voigt, T. Sander, M. Cercignani and P. Krüger, "Improved

spatio-temporal measurements of visually evoked fields using optically-pumped magnetometers," *Scientific Reports,* vol. 11, 2021.

[11] A. Mouraux and G. D. Ianetti, "Across-trial averaging of event-related EEG responses and beyond," *Magn Reson Imaging,* vol. 26, no. 7, pp. 1041-1054, 2008.

[12] W. van Drongelen, "Signal Averaging," in *Signal Processing for Neuroscientists*, Academic Press, 2007, pp. 55-70.

[13] A. Hyvärinen and E. Oja, "Independent component analysis: algorithms and applications," *Neural Networks,* vol. 13, no. 4-5, pp. 411-430, 2000.

[14] F. Pedregosa, G. Varoquaux, A. Gramfort, V. Michel, B. Thirion, O. Grisel, M. Blondel, P. Prettenhofer, R. Weiss, V. Dubourg, J. Vanderplas, A. Passos, D. Cournapeau, M. Brucher, M. Perrot and E. Duchesnay, "Scikit-learn: Machine Learning in Python," *Journal of Machine Learning Research,* vol. 12, pp. 2825--2830, 2011.

[15] G. James, D. Witten, T. Hastie, R. Tibshirani and J. Taylor, An Introduction to Statistical Learning: with Applications in Python, Springer, 2023.

[16] C. Böck, L. Meier, S. Kalb, M. Vosko, T. Tschoellitsch, M. Huemer and J. Meier, "Machine Learning Based Color Classification by Means of Visually Evoked Potentials," *Applied Sciences,* vol. 11, no. 24, 2021.

[17] Ö. Türk and . M. S. Özerdem, "Epilepsy Detection by Using Scalogram Based Convolutional Neural Network from EEG Signals," *Brain Sciences,* vol. 9, no. 5, 2019.

[18] R. R. Selvaraju, M. Cogswell, A. Das, R. Vedentam, D. Parikh and D. Batra, "Grad-CAM: Visual Explanations from Deep Networks via Gradient-based Localization," *International Journal of Computer Vision,* vol. 128, p. 336–359, 2019.

[19] D. W. Sutterer, A. J. Coia, V. Sun, S. K. Shevell and E. Awh, "Decoding chromaticity and luminance from patterns of EEG activity," *Psychophysiology,* vol. 58, 2021.

[20] A. K. Bhowmik, "Sensification of computing: adding natural sensing and perception capabilities to machines," *Industrial Technology Advances,* vol. 6, 2016.

[21] Z. O'Brien, E. Joshi and H. Sharma, "Visual Object Recognition: The Processing Hierarchy of the Temporal Lobe," in *Bridging Human Intelligence and Artificial Intelligence* , Springer, 2022, pp. 197-206.

[22] B. K. Alsberg, A. M. Woodward and D. B. Kell, "An introduction to wavelet transforms for chemometricians: A time-frequency approach," *Chemometrics and Intelligent Laboratory Systems,* vol. 37, no. 2, p. 215–239, 1997.

[23] scikit-learn, "scikit-learn," github, [Online]. Available: https://github.com/scikit-learn/scikit-learn.